Aggregation of Zinc Protoporphyrin in Anodized Aluminum Oxide (AAO) Nanoporous Environments

Jin-Shyong Lin[a] (林金雄), Yu-Chying Chen[b] (陳鈺菁), Chien-Chon Chen[b] (陳建仲), Eric Wei-Guang Diau[b]* (刁維光) and Tzeng-Feng Liu[a] (劉增豐)

[a]*Department of Material Science and Engineering, National Chiao Tung University, Hsinchu 30010, Taiwan, R.O.C.*

[b]*Department of Applied Chemistry, Institute of Molecular Science and Center for Interdisciplinary Molecular Science, National Chiao Tung University, Hsinchu 30010, Taiwan, R.O.C.*

The aggregation behavior of zinc protoporphyrin (ZnPP) inside nanoporous environments of anodized aluminum oxide (AAO) has been investigated through observation of the variation of UV/visible absorption and emission spectra of the system. The Soret band in the absorption spectrum of ZnPP/AAO thin-film samples becomes much broader than that observed for ZnPP/THF solutions, and the relative intensity of the Q band is distinctly enhanced for the former. The broad Soret band overlaps the enhanced Q band increasingly as the degree of aggregation increases with increasing duration of immersion, with initial concentration of ZnPP/THF solutions, or with decreasing pore size of AAO nanotubes. A strong excitonic coupling between the Soret and Q transition dipoles causes the absorption spectrum of the ZnPP/AAO system to cover the entire visible spectral region. Emission spectra of ZnPP/AAO samples in the steady state contain multiple resolvable components assigned to monomer, dimer and higher aggregates. The observed systematic variation of emission spectra of ZnPP/AAO samples is consistent with the observation in absorption spectra of the system and reflects the significance of aggregation of ZnPP in a specific nanoporous environment.

Keywords: AAO; Aggregation; Excitonic coupling; Porphyrin; Solar energy conversion.

INTRODUCTION

Porphyrins play an important role in living organisms.[1] The power of porphyrins to absorb light has been used in the design of artificial light-harvesting systems,[2] making molecules of this type a prospective candidate for future applications of renewable energy such as dye-sensitized solar cells and conversion of solar energy.[3-5] The UV/visible spectrum of a typical porphyrin molecule features only an intense sharp absorption about 400 nm (the so-called B or Soret band), whereas in the region 500-700 nm the absorption of the Q band is typically weak. According to reports,[6,7] the Q-band transition can borrow intensity from the intense Soret-band transition in porphyrin aggregates; such aggregates thereby become a prospective photosensitizer for solar energy conversion.

The effect of aggregation of porphyrin in aqueous solutions has been extensively investigated: porphyrin aggregates are formed at large porphyrin concentrations,[8] on addition of inorganic salt,[8,9] on variation of pH,[10,11] with cationic surfactants,[12] or on binding to DNA.[13] For protoporphyrin IX as an example,[11] a monomer prevails in a pH range 0-3, dimer for pH > 8, and higher aggregates are present in the pH range 3-7. At an intermediate pH condition, a broadened and split Soret band was observed in a range 300-500 nm in the UV/visible spectrum, but fluorescent emission was substantially quenched under these conditions. An explanation of these split Soret bands observed for such aggregates involves π-π stacking interactions with strong hydrophobic contacts edge to edge.[11]

Here we report the first demonstration of a significant effect of aggregation of porphyrins in nanoporous environments from the observation of the variation of UV/visible absorption and fluorescent emission spectra of the system.

Special Issue for the 4th Asia Photochemistry Conference, January 5~10, 2005, Taipei, Taiwan, R.O.C.

* Corresponding author. Fax: +886-03-572-3764; E-mail: diau@mail.ac.nctu.edu.tw

We prepared samples as thin films on a nanoporous substrate of anodized aluminum oxide (AAO) immersed for varied periods in a solution of zinc protoporphyrin (ZnPP; the chemical structure is indicated in Chart 1)/THF; the aggregation behavior of porphyrin varied as a function of its concentration. We found similarly that molecular aggregation of ZnPP molecules inside AAO nanotubes is controllable according to the initial concentration of the ZnPP/THF solution, the duration of immersion of the AAO substrate in the solution, and the average size of pores of AAO nanotubes. We observed strong excitonic coupling between B and Q transitions in UV/visible absorption spectra of ZnPP aggregates formed inside AAO nanotubes with two different sizes (15 nm and 70 nm). The B-band absorption became significantly broadened and the Q-band absorption became distinctly enhanced upon aggregation of ZnPP molecules inside these AAO nanoporous environments. The emission spectra of ZnPP/AAO samples in a steady state contain multiple resolvable components assigned to monomer, dimer and higher aggregates. Because this strong excitonic coupling between B and Q bands has made the absorption spectrum of the system cover the entire visible spectral region so broadly, our experiments provide important evidence for a porphyrin/nanoporous system to be considered a prospective material in future applications for a solar cell and for conversion of solar energy.

Chart 1 Chemical Structures of ZnPP and ZnOEP

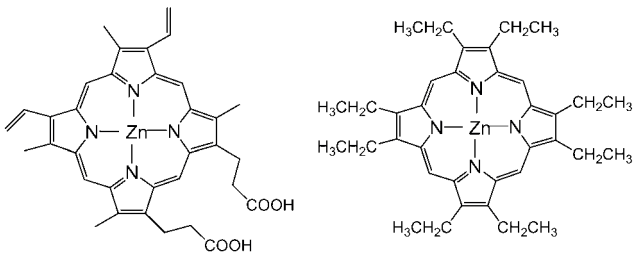

ZnPP ZnOEP

EXPERIMENTS

Preparation of AAO Nanotubes

Aluminum foil (Al, 99.7% purity) with dimensions 50 $cm^2 \times 0.3$ mm was cleaned with ethanol (C_2H_5OH, 95%) in an ultrasonic bath. To decrease grain boundaries and to increase the size of crystalline grains in the Al specimen, we annealed the specimen for 1 hr at 550 °C in a furnace in air. To diminish surface roughness, we performed electropolishing (EP) in a solution consisting of 15% perchloric acid ($HClO_4$, 70%), 70% ethanol (99.5%), and 15% butyl cellosolve ($CH_3(CH_2)_3OCH_2CH_2OH$, 85%), with stirring for 6 min at 12 °C at an applied voltage 32 V.[14,15] The flat Al surface was formed after EP and the specimen was ready for further treatments to prepare the anodized aluminum oxide substrates described as follows.

To vary the diameter d of AAO nanotubes, we performed two anodization procedures.[16] For an AAO nanotube of diameter 10-15 nm, we treated the flat Al substrate in a 10% solution of sulfuric acid (H_2SO_4, 98%) at 10 °C for 10 min and an applied voltage 18 V. For an AAO nanotube with d = 30-40 nm we treated the flat Al substrate in a 3% solution of oxalic acid ($C_2H_2O_4$, 99.9%) at 20 °C and applied voltage 40 V.[17,18] Figs. 1A-C show SEM images of AAO nanotubes produced from the former treatments and Figs. 1D-F show corresponding SEM images of AAO nanotubes from the latter treatments. As pores are created randomly on an AAO surface, the initial pore arrangement is irregular. Figs. 1A and D show the initial patterns of AAO nanotubes with the former and latter treatments, respectively, but the bottom pores are more regular than the top pores of these nanotubes. For this reason we obtained a regular pattern by removing AAO with wet chemical etching using a mixture containing 6 wt % phosphoric acid (H_3PO_4, 98%) and 1.8 wt % chromic acid (CrO_3, 95%) at 60 °C for 40 min.[16] Patterns that are replicas of the hexagonal pore array are preserved on the fresh Al surface, as shown in Figs. 1B and E for treatments according to the former and latter procedures, respectively. After the second anodization for 4 hr under the same conditions as the first anodization, AAO nanotubes grew based on these patterns. The arrangement of the AAO pattern after the second anodization (Figs. 1C and F) is evidently much more ordered than the pattern after the first anodization (Figs. 1A and D). Ordered AAO nanotubes with d = 15 nm and 74 μm thickness can thus be formed on treatment with sulfuric acid (Figs. 2A). To obtain smooth and ordered pores of AAO nanotubes on treatment with oxalic acid, we annealed the AAO substrates in an air furnace at 550 °C for 8 hr, then widened the pores in 5% phosphoric acid solution at 25 °C for 2 hr. As a result, AAO nanotubes with d = 70 nm and thickness 51 μm were produced, as clearly shown in Fig. 2B.

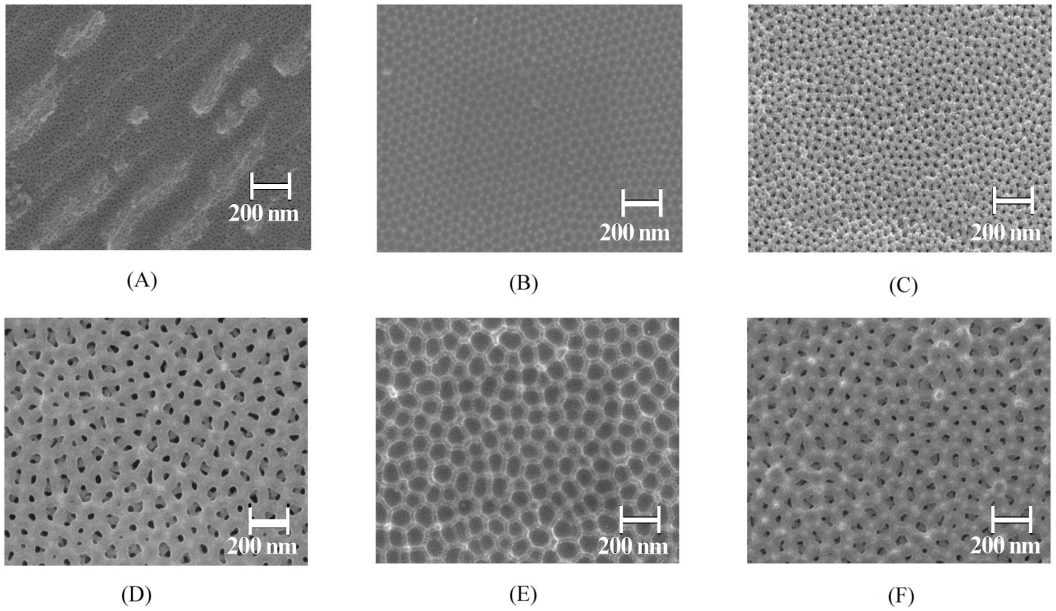

Fig. 1. SEM images of AAO from anodization obtained from 10 vol % sulfuric acid (A-C) and 3 wt % oxalic acid (D-F) treatments. (A) and (D) show the initial AAO surface after a first anodization, (B) and (E) show the pattern of order on the Al surface after removal of AAO by wet chemical etching, and (C) and (F) show the AAO surface after a second anodization.

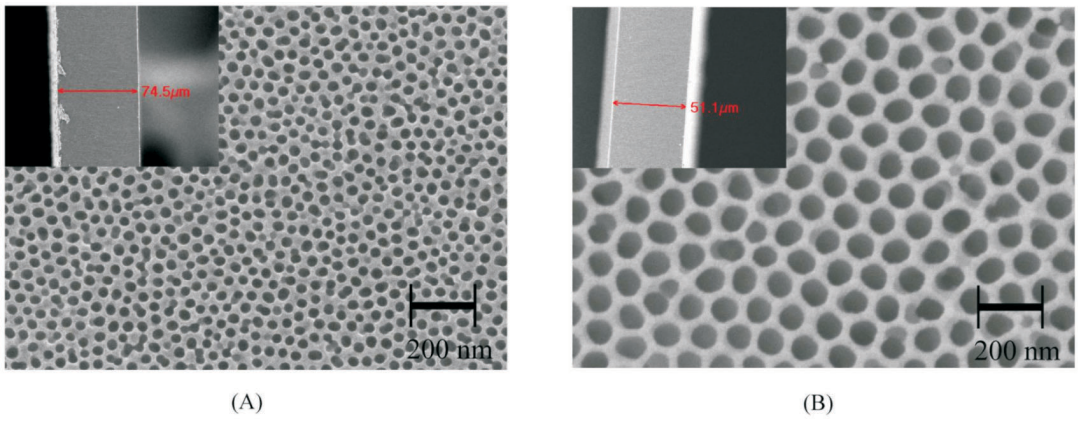

Fig. 2. SEM images of AAO after two-step anodization and pore widening: (A) AAO with pore size 15 nm and thickness 74.5 μm formed in 10 vol % H_2SO_4 electrolyte; (B) AAO with pore size 70 nm pore size and thickness 51.1 μm formed in 3 wt % $(COOH)_2$ electrolyte.

Materials

ZnPP (Chart 1, Sigma-Aldrich, purity > 95%) was used without further purification. ZnPP was dissolved in THF (Merck, spectral grade) to form a solution in three initial concentrations C_i – 4.8×10^{-6} M, 4.8×10^{-5} M and 4.8×10^{-4} M. The AAO nanoporous substrates (disk shape, diameter 1 cm) were immersed in these ZnPP/THF solutions of constant volume (~5 mL) in a closed container at room temperature. After a period t_i of immersion, we took the ZnPP/AAO nanoporous substrates from the solutions and rinsed them carefully several times with pure THF to remove physically adsorbed ZnPP molecules on the surface or inside the nanotubes before the spectral measurements.

Spectral Measurements

UV/visible absorption spectra of ZnPP/AAO samples

as thin films were measured with a composite CCD spectrometer (HR4000CG-UV-NIR, Ocean Optics) coupled with a deuterium/tungsten/halogen lamp (DH-2000, Ocean Optics) via a fiber (Y-shape, R600-UV, Ocean Optics) for reflection probes. The measurements were performed in two steps: first, the reflection spectrum of the blank AAO substrate was recorded as R_λ; second, the reflection spectrum of the ZnPP/AAO sample was recorded as S_λ. We obtained the absorption spectrum (A_λ) from the relation $A_\lambda = -\log (R_\lambda/S_\lambda)$. Fluorescence emmision spectra were obtained with another composite CCD spectrometer (USB2000FLG, Ocean Optics) with an excitation lamp containing a pulsed diode laser head (LDH-P-C-440, PicoQuant) coupled with a laser diode driver (PDL-800B, PicoQuant) that produces excitation pulses at 435 nm with an average power ~300 μW.

RESULTS AND DISCUSSION

Formation of ZnPP Aggregates inside AAO Nanotubes

Fig. 3 shows UV/visible spectra of ZnPP under four conditions. The absorption spectrum of the ZnPP/THF solution ($C_M = 4.8 \times 10^{-6}$ M) has two features corresponding to one symmetry-allowed transition, known as the B or Soret band, with a maximum at 420 nm, and two symmetry-forbidden transitions, with maxima at 545 and 580 nm, known as Q(0,0) and Q(0,1) bands, respectively. When the

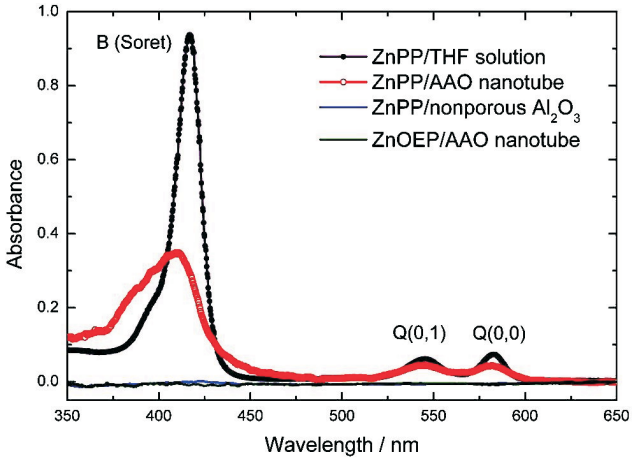

Fig. 3. UV/visible absorption spectra of ZnPP in various environments as indicated; experimental conditions: $C_i = 4.8 \times 10^{-6}$ M, $t_i = 20$ hr, and $d = 15$ nm.

AAO nanoporous substrates ($d = 15$ nm) were immersed in ZnPP/THF solution for 20 hr, we found that the UV/visible spectrum of the ZnPP-sensitized AAO thin-film sample showed spectral features different from those of ZnPP in solution: in particular the B band of the spectrum for the ZnPP/AAO sample becomes much broader than for the solution, as shown in Fig. 3. To prove that the above spectral observation of the ZnPP/AAO sample is due to ZnPP aggregates inside AAO nanotubes, we performed two control experiments.

First, the bulk nonporous aluminum-oxide substrate was immersed in the ZnPP/THF solution under the same conditions; the UV/visible spectrum of this ZnPP/Al_2O_3 nonporous substrate shows only a minute absorbance in the region of the B-band absorption area of ZnPP (shown as a lower trace in Fig. 3). Hence the fraction of ZnPP sensitized on the AAO surface outside the nanotube is negligible, whereas, because the surface area inside the nanotubes is large, most ZnPP is located there.

Second, the AAO nanoporous substrate was immersed in a ZnOEP/THF solution under the same conditions. ZnOEP is another porphyrin molecule having a molecular structure similar to that of ZnPP but without the carboxylic acid group (Chart 1). After rinsing many times with pure THF solvent, the color of the ZnOEP/AAO sample disappeared and the corresponding UV/visible spectrum showed essentially no absorption in the entire spectral region (shown as a lower trace in Fig. 3). The interaction between ZnOEP and AAO nanotubes is evidently so weak that no ZnOEP molecules remain inside the AAO nanotubes after rinsing with the solvent, but the ZnPP molecules attached inside AAO nanotubes can not be rinsed out with a solvent. We thus conclude that ZnPP molecules originally dissolved in the solution diffused into the AAO nanotubes to reside inside such a typical nano-environment with strong chemical binding via the carboxylate group as a bridge at the interface between Al_2O_3 substrate and the ZnPP molecule.

According to results obtained from our control experiments, we have proved that the observed specific UV/visible spectra of ZnPP/AAO samples are due to formation of ZnPP aggregates inside the AAO nano-structural environment.

Aggregation Effect as a Function of t_i, C_i, and d

The amount of ZnPP molecules inside AAO nanotubes is controllable through the duration t_i of immersion,

the initial concentration C_i of the ZnPP/THF solution, and the pore size d of AAO nanotubes. Figs. 4A-C show UV/visible spectra of ZnPP/AAO nanoporous substrates as a function of period of immersion at $C_i = 4.8 \times 10^{-6}$ M, 4.8×10^{-5} M and 4.8×10^{-4} M, respectively. For $C_i = 4.8 \times 10^{-6}$ M, the absorbance of both B and Q bands evidently increases gradually with increasing duration of immersion. For $C_i = 4.8 \times 10^{-5}$ M, the B band begins to broaden and the Q bands begin to grow at $t_i = 1$ hr; the Q bands continue to grow with prolonged immersion but the absorbance of the B band does not alter significantly. For $C_i = 4.8 \times 10^{-4}$ M, the B band has already become broadened with enhanced Q-band absorption at $t_i = 15$ min; the absorbance of the broad B band decreases with increasing absorption in the Q band at greater t_i. After immersion for two days ($t_i = 48$ hr), the maximum absorbance of the Q bands even exceeds the maximum absorbance of the B band at $C_i = 4.8 \times 10^{-4}$ M (Fig. 4C). In contrast, the effect of aggregation becomes less significant when the average pore diameter of the AAO nanotubes is enlarged (i.e., $d = 70$ nm), as shown in Figs. 5A-C for UV/visible spectra observed at $C_i = 4.8 \times 10^{-6}$ M, 4.8×10^{-5} M and 4.8×10^{-4} M, respectively.

These observations for the formation of ZnPP aggregates inside the AAO nano-structural environment show several important spectral features differing from the case of the free solvent environment; they are summarized in the following three major points. First, the Soret band of the absorption spectrum of ZnPP/AAO thin-film samples is much broader than that observed for ZnPP/THF solutions. Second, the relative absorbance of the Q band of the former is distinctly enhanced with respect to that of the latter. Third, a red tail of the Q band emerges at larger C_i and greater t_i when ZnPP aggregation becomes highly significant. We therefore conclude that the broad B band overlaps increasingly the enhanced Q band with increasing extent of aggregation upon increasing the duration t_i of immersion, increasing the initial concentration C_i of ZnPP/THF solu-

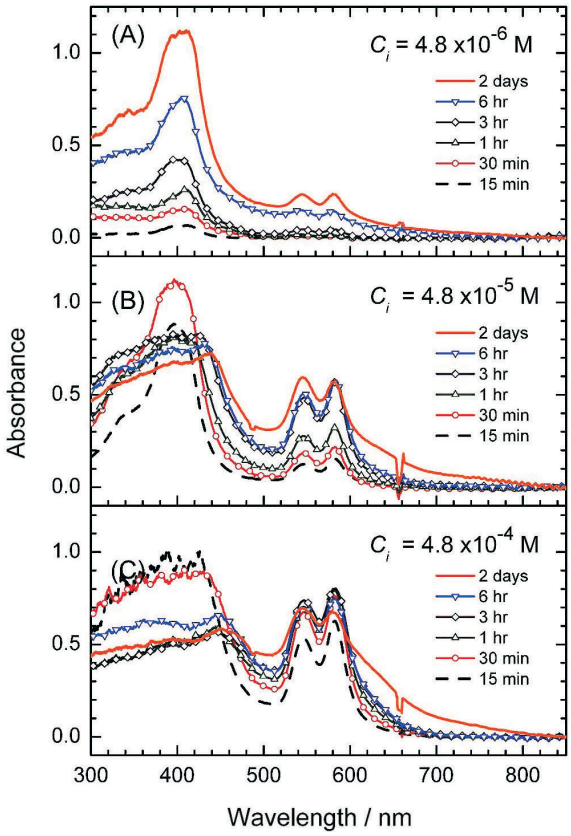

Fig. 4. UV/visible absorption spectra of ZnPP/AAO (d = 15 nm) as a function of duration t_i of immersion for C_i = (A) 4.8×10^{-6} M; (B) 4.8×10^{-5} M; (C) 4.8×10^{-4} M.

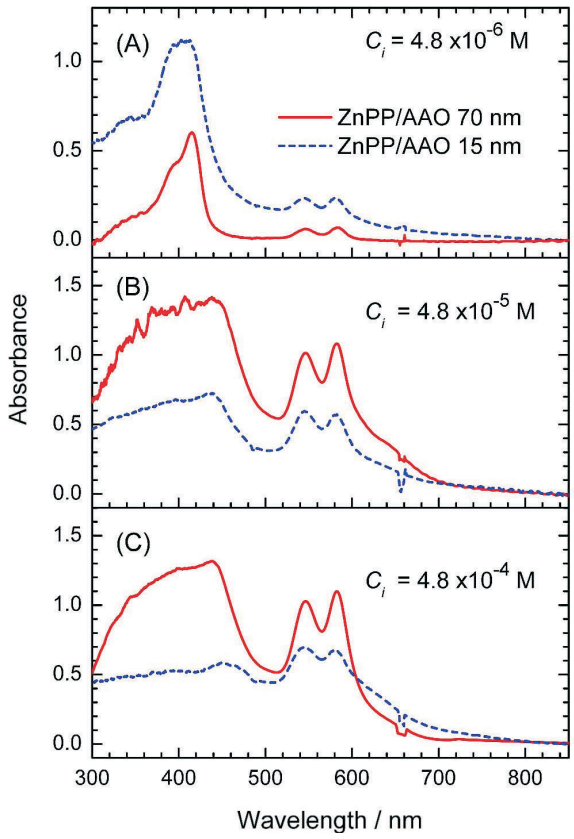

Fig. 5. UV/visible absorption spectra of ZnPP/AAO with d = 70 nm at t_i = 48 hr for C_i = (A) 4.8×10^{-6} M; (B) 4.8×10^{-5} M; (C) 4.8×10^{-4} M; spectra of ZnPP/AAO with d = 15 nm are shown in dashed curves for comparison.

tions, or decreasing the pore diameter d of the AAO nanotubes.

The absorption spectrum of a porphyrin derivative becomes distinctly altered upon aggregation;[10,11] the enhanced intensity in the Q-band region is "borrowed" from the Soret band by excitonic coupling between the Soret and Q transition dipoles.[7] This mechanism perfectly explains our observation that the excitonic interaction between the Soret and Q bands systematically increases with increasing t_i or C_i, or decreasing d. Such a pronounced effect for ZnPP aggregates in the nano-structural environment causes the absorption spectra of ZnPP/AAO samples to cover the entire visible spectral region; this effect is unachievable with conventional approaches involving altering either the pH or the salt concentration in aqueous solutions.[9-11]

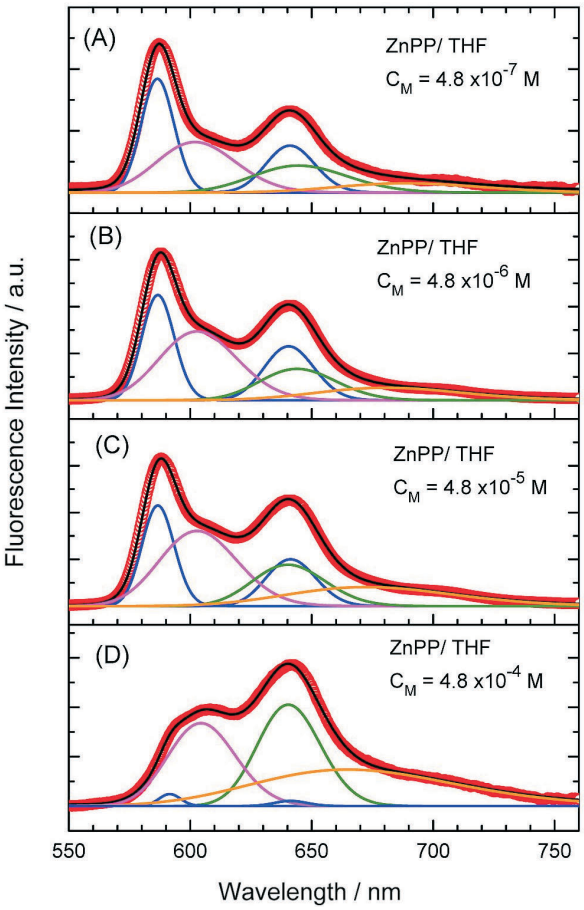

Fig. 6. Fluorescent emission spectra of ZnPP/THF solutions obtained at C_M = (A) 4.8×10^{-7} M; (B) 4.8×10^{-6} M; (C) 4.8×10^{-5} M; (D) 4.8×10^{-4} M. The circles are raw data and the solid curves are the theoretical fits of the spectra; the curves under the spectral profiles are the Gaussian components deconvoluted from the fit: the two peaked curves represent emission from the ZnPP monomer, the middle curve for the ZnPP dimer, and both curves in the greater wavelength region for lower and higher aggregates, respectively.

Aggregation Effect as Observed from Emission Spectra

To understand the effect of aggregation of ZnPP in a free solvent environment, we recorded spectra of ZnPP dissolved in solutions of varied concentration. Figs. 6A-D show emission spectra in a steady state of ZnPP at four concentrations in a range 4.8×10^{-7}-4.8×10^{-4} M. All emission spectra were fitted with several Gaussian components. According to the results obtained from aqueous solutions at varied pH,[11] we assigned the deconvoluted Gaussian components of each spectrum to contributions from several sources: the two curves corresponding to the peaks of the spectrum pertain to the emission arising from the ZnPP monomer and the middle curve pertains to emission due to the ZnPP dimer; the components at greater wavelengths are due to ZnPP lower and higher aggregates, respectively. Aggregation of the ZnPP molecules is unavoidable even in the most dilute solution, for which $C_M = 4.8 \times 10^{-7}$ M. The extent of aggregation varies systematically as a function of concentration. For a solution at $C_M = 4.8 \times 10^{-4}$ M (Fig. 6D), the contribution of the monomer is nearly negligible; the emission spectrum is contributed mostly by dimer and lower and higher aggregates.

We investigated the effect of aggregation of ZnPP inside AAO nanotubes through emission spectra of the ZnPP/AAO system in a steady state; the results obtained at $t_i = 48$ hr appear in Fig. 7. Emission spectra for varied environments show spectral profiles that differ because of varying contributions by ZnPP aggregates. We therefore deconvoluted the spectral profiles of ZnPP/AAO samples into several Gaussian components using the same fitting procedure as for the ZnPP/THF solution. For the spectrum obtained at $d = 15$ nm and $C_i = 4.8 \times 10^{-6}$ M, at least three comparable components, one representing ZnPP dimer and the other two representing ZnPP aggregates, are required to fit the spectral profiles shown in Fig. 7A. For $d = 70$ nm and $C_i = 4.8 \times 10^{-6}$ M, Fig. 7B shows that the contribution of monomer is enhanced with the other components correspondingly less significant; the second feature of the monomer is unresolved because it is heavily embedded under the major component of aggregates. When the initial concentration of

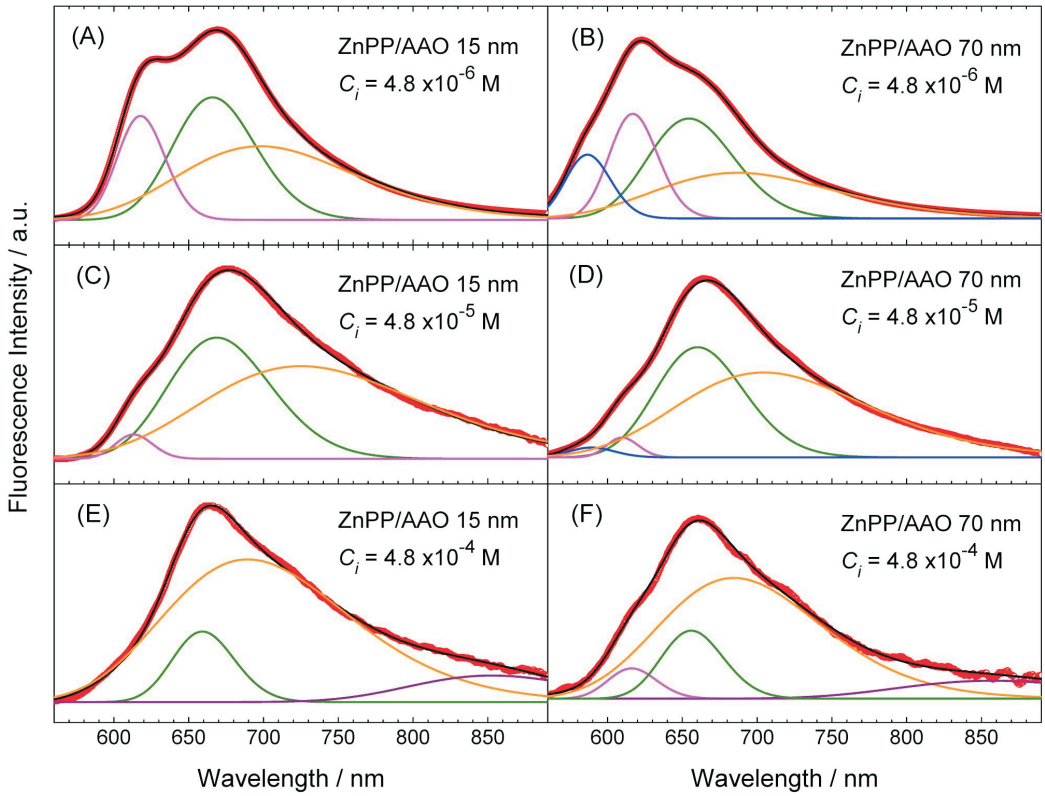

Fig. 7. Fluorescent emission spectra of ZnPP/AAO nanoporous samples obtained at (A) $C_i = 4.8 \times 10^{-6}$ M and $d = 15$ nm; (B) $C_i = 4.8 \times 10^{-6}$ M and $d = 70$ nm; (C) $C_i = 4.8 \times 10^{-5}$ M and $d = 15$ nm; (D) $C_i = 4.8 \times 10^{-5}$ M and $d = 70$ nm; (E) $C_i = 4.8 \times 10^{-4}$ M and $d = 15$ nm; (F) $C_i = 4.8 \times 10^{-4}$ M and $d = 70$ nm. The representation for the fits of the spectra is the same as in Fig. 6 except that the curves at greatest wavelengths pertain to other aggregates.

immersion is increased to $C_i = 4.8 \times 10^{-5}$ M, the contribution of both aggregate components becomes significantly larger than that of the monomer and dimer for spectra with both $d = 15$ nm (Fig. 7C) and $d = 70$ nm (Fig. 7D). At $C_i = 4.8 \times 10^{-4}$ M, not only does a second aggregate component become a major part of the spectrum but also a new component emerges at greater wavelengths. This observed systematic variation of emission spectra of ZnPP/AAO samples as a function of C_i and d is consistent with the observation of absorption spectra of the system and reflects the significance of aggregation of ZnPP in the specific nanoporous environments.

CONCLUDING REMARKS

Based on observations of the variation of UV/visible absorption spectra and fluorescent emission spectra, we have demonstrated a significant effect of aggregation of ZnPP inside AAO nanoporous environments. Molecular aggregation of ZnPP molecules inside AAO nanotubes is controllable through the initial concentration of the ZnPP/THF solution, the duration of immersion of the AAO substrate in the solution, and the average pore size of the AAO nanotubes. We have observed strong excitonic coupling between B and Q transitions in UV/visible absorption spectra of ZnPP aggregates formed inside AAO nanotubes of varied pore sizes (d = 15 nm vs. 70 nm). The effect of aggregation is attributed to transfer of intensity from the B- to the Q-band region that is mediated by an excitonic coupling between B and Q transition dipoles.[7] Emission spectra of the ZnPP/AAO samples in a steady state possess multiple resolvable components assigned to monomer, dimer and other aggregates.

This work has an important impact for the porphyrin/nanoporous system to be regarded as a prospective material in applications as a solar cell. The effect of excitonic coupling of B and Q bands of porphyrin aggregates inside the nanoporous environment is much more significant than in aqueous solutions at intermediate pH.[11] Such a strong ef-

fect of aggregation causes the absorption spectrum of the porphyrin/nanoporous system to cover the entire visible spectral region. The system can thus be utilized as an efficient photosensitizer to examine the photovoltaic effect in applications for renewable energy such as a dye-sensitized solar cell or the conversion of solar energy.

ACKNOWLEDGEMENT

The National Science Council of the Republic of China provided financial support under contract 94-2113-M-009-016.

Received May 3, 2005.

REFERENCES

1. Milgrom, L. R. *The Colours of Life*; Oxford University Press Inc.: New York, 1997.
2. Balzani, L.; Credi, A.; Venturi, M. *Molecular Devices and Machines*; Wiley-VCH: Germany, 2003; and related references therein.
3. Kalyanasundaram, K.; Vlachopoulos, N.; Krishnan, V.; Monnier, A.; Grätzel, M. *J. Phys. Chem.* **1987**, *91*, 2342.
4. Tachibana, Y.; Haque, S. A.; Mercer, I. P.; Durrant, J. T.; Klug, D. R. *J. Phys. Chem. B* **2000**, *104*, 1198.
5. Grätzel, M. *Nature* **2001**, *414*, 338.
6. Kano, Hideaki; Saito, T.; Kobayashi, T. *J. Phys. Chem. B* **2001**, *105*, 413.
7. Zimmermann, J.; Siggel, U.; Fuhrhop, Roder, B. *J. Phys. Chem. B* **2003**, *107*, 6019.
8. Shelnutt, J. A.; Dobry, M. M.; Satterlee, J. D. *J. Phys. Chem.* **1984**, *88*, 4980.
9. Kano, K.; Fukuda, K.; Wakami, H.; Nishiyabu, R.; Pasternack, R. F. *J. Am. Chem. Soc.* **2000**, *122*, 7494.
10. Inamura, I.; Uchida, K. *Bull. Chem. Soc. Jpn.* **1991**, *64*, 2005.
11. Scolaro, L. M.; Castriciano, M.; Romeo, A.; Patane, S.; Cefali, E.; Allegrini, M. *J. Phys. Chem. B* **2002**, *106*, 2453.
12. Maiti, N. C.; Mazumdar, S.; Periasamy, N. *J. Phys. Chem. B* **1998**, *102*, 1528.
13. Pasternack, R. F.; Bustamante, C.; Collings, P. J.; Giannetto, A.; Gibbs, E. J. *J. Am. Chem. Soc.* **1993**, *115*, 5393.
14. Jessensky, O.; Muller, F. *Appl. Phys. Lett.* **1998**, *72*, 117.
15. Li, Y.; Holland, E. R.; Vac, J. *Sci. Technol. B* **2000**, *18*, 994.
16. Chen, C. C.; Chen, J. H.; Chao, C. G. *Jan. J. Appl. Phys.* **2005**, *44*, 1529.
17. Masuda, H.; Fukuda, K. *Science.* **1995**, *268*, 1466.
18. Masuda, H.; Yamada, H. *Appl. Phys. Lett.* **1997**, *71*, 2770.